

This un-edited manuscript has been accepted for publication in Biophysical Journal and is freely available on BioFast at <http://www.biophysj.org>. The final copyedited version of the paper may be found at <http://www.biophysj.org>.

**Modulation of SR Ca Release by Luminal Ca and Calsequestrin in Cardiac Myocytes:
Effects of CASQ2 Mutations Linked to Sudden Cardiac Death.**

Dmitry Terentyev^{*}, Zuzana Kubalova[†], Giorgia Valle[‡], Alessandra Nori[‡], Srikanth Vedamoorthyrao^{*}, Radmila Terentyeva^{*}, Serge Viatchenko-Karpinski^{*}, Donald M. Bers[§], Simon C. Williams[¶], Pompeo Volpe[‡], and Sandor Gyorke^{*¶}.

^{*}The Ohio State University Medical Center, Department Physiology, Davis Heart and Lung Research Institute, Columbus, Ohio; [†]Institute of Molecular Physiology and Genetics, Slovak Academy of Sciences, Bratislava, Slovak Republic; [‡]University of Padova, Italy; [§]Loyola University Chicago, Maywood, Illinois; [¶]Texas Tech University, Lubbock, Texas.

Short title: Calsequestrin mutations in CPVT.

[¶]Corresponding author:

Sandor Gyorke, Ph.D.

Professor of Physiology and Cell Biology

Associate Director

Dorothy Davis Heart and Lung Research Institute

Ohio State University

473 West 12th Avenue

Columbus, OH 43210-1252

e-mail: sandor.gyorke@osumc.edu

ABSTRACT

Cardiac calsequestrin (CASQ2) is an intra-sarcoplasmic reticulum (SR) low-affinity Ca-binding protein, mutations in which are associated with catecholamine-induced polymorphic ventricular tachycardia (CPVT). To better understand how CASQ2 mutants cause CPVT, we expressed two CPVT-linked CASQ2 mutants, a truncated protein (at G112+5X, CASQ2^{DEL}) or CASQ2 containing a point mutation (CASQ2^{R33Q}), in canine ventricular myocytes and assessed their effects on Ca handling. We also measured CASQ2-CASQ2 variant interactions using fluorescence resonance transfer (FRET) in a heterologous expression system, and evaluated CASQ2 interaction with triadin. We found that expression of CASQ2^{DEL} or CASQ2^{R33Q} altered myocyte Ca signaling through two different mechanisms. Overexpressing CASQ2^{DEL} disrupted the CASQ2 polymerization required for high capacity Ca binding, while CASQ2^{R33Q} compromised the ability of CASQ2 to control ryanodine receptor (RyR2) channel activity. Despite profound differences in SR Ca buffering strengths, local Ca release terminated at the same free luminal [Ca] in control cells, cells overexpressing wild type CASQ2 and CASQ2^{DEL} – expressing myocytes, suggesting that a decline in [Ca]_{SR} is a signal for RyR2 closure. Importantly, disrupting interactions between the RyR2 channel and CASQ2 by expressing CASQ2^{R33Q} markedly lowered the [Ca]_{SR} threshold for Ca release termination. We conclude that CASQ2 in the SR determines the magnitude and duration of Ca release from each SR terminal by providing both a local source of releasable Ca and by effects on luminal Ca-dependent RyR2 gating. Furthermore, two CPVT-inducing CASQ2 mutations, which cause mechanistically different defects in CASQ2 and RyR2 function, both lead to increased diastolic SR Ca release events and exhibit a similar CPVT disease phenotype.

Key words: Calsequestrin, Ryanodine Receptor, Sarcoplasmic Reticulum, Ca-Induced Ca Release, Catecholaminergic Polymorphic Ventricular Tachycardia.

INTRODUCTION.

The sarcoplasmic reticulum (SR) is a Ca release and storage organelle that plays a key role in regulating muscle contraction and relaxation. In cardiac muscle, the SR Ca store provides the majority of Ca required for contractile activation and it enables the myocardium to relax by resequestering Ca (1). The release of Ca from the SR, which takes place through specialized SR Ca release channels (ryanodine receptors, RyR2), is initiated by a relatively small Ca influx through sarcolemmal Ca channels during depolarization, a process known as Ca-induced Ca release (CICR). Ca release to the cytosol is accompanied by a reciprocal decline in intra-SR [Ca]; however, only a fraction of the total Ca is normally released from the SR (2, 3) due to RyR2 closure which terminates Ca release (4, 5). This RyR2 deactivation is thought to contribute to subsequent refractoriness of Ca release, which may limit diastolic SR Ca release and enhance CICR stability. It has been suggested that release termination and refractoriness might be caused by a decline in $[Ca]_{SR}$ inhibiting RyR2 activity (6-9) (i.e. luminal Ca dependent-deactivation (6)); however, the specific molecular steps involved in these processes remain to be defined.

Calsequestrin (CASQ) is a low-affinity, high-capacity Ca binding protein located within the SR (10, 11). CASQ is detected as electron-dense filamentous matrices localized in the junctional SR (jSR) and is almost completely absent from the SR longitudinal network in both skeletal and cardiac muscle (isoforms CASQ1 and CASQ2, respectively) (12). The filamentous matrices are composed of linear oligomers formed by CASQ monomers and dimers at Ca concentrations above 10 mM (13-15). The unique distribution and structural organization of CASQ are believed to be of key physiological importance although the specific modes of operation of this protein only begin to emerge. Due to their proximity to RyRs the condensed CASQ matrices are thought to provide the pool of releasable Ca to activate myocyte contraction. In this regard, condensed CASQ represents the high Ca binding capacity form of the protein that possesses at least twice the Ca binding capacity of CASQ monomers in both skeletal and cardiac muscle (15). CASQ condensation reportedly involves head-to-tail oligomerization that occurs through front-to-front and back-to-back dimerization contacts involving the N- and C-terminal regions of the protein, respectively (13-15). In addition to serving as a Ca storage site, cardiac calsequestrin (CASQ2) has been shown to regulate RyR2 activity more directly via protein-protein interactions involving triadin (TRD) and junctin (Jn) (16). In particular, it has been proposed that CASQ2 mediates the responsiveness of the RyR2 channel to luminal Ca by serving as a luminal Ca sensor (17).

Consistent with a critical role for calsequestrin in maintaining myocardial function, genetic defects in CASQ2 have been linked to catecholaminergic polymorphic ventricular tachycardia (CPVT), a familial form of arrhythmia and sudden cardiac death inducible by catecholamine infusion and exercise (18-20). Seven distinct mutations within the CASQ2 gene have been linked to CPVT so far (<http://www.fsm.it/cardmoc/>) (18-21). Initial characterization of these mutations has suggested that they act by disrupting normal SR Ca handling, thereby leading to premature recovery of SR Ca release from a luminal Ca-dependent refractory state and causing spontaneous after-Ca transients and arrhythmogenic delayed after-depolarizations (DADs) (22, 23). However, the specific details as to how different mutations, potentially affecting different aspects of CASQ2 function, lead to the same pathophysiological phenotype remains to be determined.

The goal of the present study was to investigate the mechanisms of action of two recently described CPVT-related CASQ2 mutations (referred to here as CASQ2^{R33Q} and CASQ2^{DEL}) on

Ca signaling in cardiac myocytes. CASQ2^{R33Q} is derived from a CASQ2 allele carrying a missense mutation at nucleotide 99 (G99A), which results in the substitution of a glutamine for an arginine residue at position 33 (20). CASQ2^{DEL} is derived from a CASQ2 allele in which nucleotides 339-354 have been deleted (Del.339-354) and results in a frameshift following the codon for amino acid 112 and introduction of a stop codon after a further five amino acids (G112+5X) (21). Although expression of both of these CASQ2 variants led to arrhythmogenic Ca release, the introduction of one variant was associated with a loss of function, whereas the other with a gain of function effects on SR Ca release (20, 21). To define the mechanisms of action of these mutants on Ca signaling we monitored intracellular Ca cycling in permeabilized myocytes overexpressing wild type (WT) or mutant forms of CASQ2 by simultaneously imaging Ca changes in the cytosolic and SR compartments during both global (Ca waves) and localized Ca release (Ca sparks). We also performed fluorescence resonance transfer (FRET) measurements and used in vitro affinity binding assays to assess the effects of the mutations on the ability of CASQ2 to polymerize and interact with TRD. Our results showed that expression of CASQ2^{DEL} and CASQ2^{R33Q} altered SR Ca signaling through two different mechanisms: by disrupting CASQ2 polymerization required for high capacity Ca binding and by altering luminal-Ca dependent modulation of the RyR2 channel by CASQ2. Our studies provided new evidence for the role of Ca in dynamic control of SR Ca release and showed that CASQ2 plays a dual role as a local source of releasable Ca and a luminal Ca sensor for the RyR2 channel.

MATERIALS AND METHODS.

Plasmid Construction.

The coding sequences of the enhanced yellow fluorescent protein (EYFP) and enhanced cyan fluorescent protein (ECFP) were isolated from the bacterial expression vectors pEYFP and pECFP (Clontech) by digestion with *Bam*HI and *Not*I. These inserts were ligated into the backbone of the pDsRed-N1 plasmid (Clontech), from which the DsRed protein coding region had been removed using the same enzymes. Canine CASQ2 sequences encoding amino acids 1-343, 1-112, or 1-343 (R33Q) were amplified by PCR from pSHUTTLE plasmids carrying either the full length coding sequence (22) or the sequence containing the R33Q mutation (20). The PCR primers were designed to introduce a *Sal*I site at the 5' end of the amplified sequence and a *Bam*HI site at the 3' end. The sequences of the three primers are as follows: primer for insertion of *Sal*I site prior to amino acid 1: GGCGTCGACGCCATGAAGAGAACACACCTG; insertion of *Bam*HI site following amino acid 112: GGCGGATCCCCTTCTTCATCAAACC, insertion of *Bam*HI site following amino acid 343: GGCGGATCCATCCAGACACTGTCGGC. The PCR products were subcloned and sequenced to ensure accurate amplification. Each insert was subsequently removed with *Sal*I and *Bam*HI and inserted into the EYFP and ECFP-containing plasmids described above.

Ca Imaging.

Intracellular Ca imaging was performed by using an Olympus Fluoview 1000 laser scanning confocal microscope equipped with an Olympus 60X 1.4 N.A. oil objective. Canine ventricular myocytes were enzymatically isolated as described previously (24), in accordance with the guidelines of the Ohio State University Institutional Animal Use and Care Committee. Isolated cells were infected with adenoviruses encompassing human WT or mutant CASQ2s at MOI 100 and kept in culture media for 48 hours at 5% CO₂ / 95% air at 37⁰C as described previously (20-

22). Culture media contained: Media 199M; 5 mM creatine; 5 mM taurine; 25 mM NaHCO₃, 5 mM HEPES, gentamicin 1 µg/ml, penicillin 10 u/ml, streptomycin 10 µg/ml, pH 7.3. To simultaneously monitor the intra-SR and cytosolic Ca levels, myocytes were initially loaded with Fluo-5N AM (10 µM, 4 hrs, 37⁰C). Subsequently, myocytes were permeabilized with saponin to remove the Fluo-5N from the cytoplasm and to introduce Rhod-2 tripotassium salt (30 µM) to the internal solution for cytosolic Ca measurements. The control intracellular solution contained (mM): 120 potassium aspartate, 20 KCl, 3 MgATP, 10 phosphocreatine, 5 u/ml creatine phosphokinase, 0.2 EGTA and 20 Hepes (pH 7.2). To evoke spontaneous Ca waves EGTA was lowered to 0.05 mM, free [Ca] ~100 nM and free [Mg]~1 mM. Fluo-5N and Rhod-2 were excited sequentially by 488- and 543-nm laser lines, and fluorescence was acquired at a rate of 5 ms per line at wavelengths of 500–530 and >560 nm, respectively. For quantitative studies, the temporal dynamics in Fluo-5N fluorescence was expressed as $F_{SR}/F_{SRmax} = (F - F_{caff})/(F_{max} - F_{caff})$, where F represents fluorescence at time t , F_{caff} represents fluorescence level of the cells after the application of 10 mM of caffeine, F_{max} represents Fluo-5N fluorescence in the presence of caffeine and 10 mM of [Ca]. $[Ca]_{SR}$ was derived as $[Ca]_{SR} = K_d(F_{SR})/(F_{SRmax}-F_{SR})$; where K_d was 400 µM (2). Data are presented as mean ± s.e. Statistical significance was tested with an unpaired Student's t test or one way ANOVA.

FRET Experiments.

Cultured (DMEM, 37⁰C) 3T3 NIH fibroblasts were lipofected (Polyfect, Qualcom) with the fusion constructs for acceptor photobleaching experiments. Fibroblasts were examined 48 hrs after transfection using an Olympus Fluoview 1000 spectral laser scanning confocal system. 512x512 16 bit XY images of the cells were taken using standard spectroscopic settings: CFP and YFP were excited sequentially frame-by-frame with the 458 and 515 nm lines, respectively, of an argon laser. The emitted fluorescence was collected at 475-500 nm for CFP and 530-630 nm for YFP. Repeated scans (10-20 frames) with unattenuated 515 nm illumination were used to photobleach YFP. CFP fluorescence intensity was measured continuously through the whole experiment and FRET efficiency was estimated using following equation: $(F_{CFPPostbleach} - F_{CFPPrebleach})/ F_{CFPPostbleach} * 100\%$. Data are reported as mean ± S.E. Statistical significance was tested with an unpaired Student's t test.

In vitro binding assay using T7-affinity column.

T7-CASQ2 constructs were generated as described previously (21). Recombinant CASQ2 proteins were expressed using pET-5a-based plasmids in BL21 (DE3) *E.coli* cells (Novagen). Large quantities of T7-CASQ2 fusion proteins were purified either by phenyl-Sepharose or T7-tag affinity column, as described previously (21). SR vesicles (Heavy SR fraction), prepared from rabbit hearts, according to Saito et al., 1984 (25) by isopycnic sucrose gradient centrifugation, were solubilized for 1 h on ice according to Zhang et al., 1997 (16), and recovered by centrifugation in a Beckman Airfuge at 105,000 x g for 1 h. Protein concentration was determined according to Lowry et al., 1951 (26). Affinity columns were prepared by immobilizing 30 µg of T7-CASQ2 fusion proteins on 100 µl of T7-affinity beads for 2 h at 4 °C. CHAPS-solubilized SR vesicles were precleared with T7-affinity beads for 2 h at 4 °C and then incubated with T7-CASQ2 affinity beads for 20 h at 4 °C. Bound proteins were eluted by boiling in the SDS sample buffer. SDS-PAGE was performed with 12.5% polyacrylamide gels. Electrophoretic transfer onto nitrocellulose membrane and Western blot with anti-TRD antibody were carried out as described (21). Polyclonal antibodies to triadin (Sh33) (27) are a generous

gift from Dr. Kevin P. Campbell (The University of Iowa, Iowa City, IA, USA). Statistical significance was tested with an unpaired Student's *t* test.

RESULTS.

Cytosolic and luminal Ca waves.

To gain insights in the mode of operation of CASQ2 in cardiac myocytes and in the underlying causes of arrhythmia caused by mutations of these proteins, we have compared the effects of ectopic expression of two recently described CPVT-associated CASQ2 variants with either gain or loss of function effects on SR Ca release, CASQ2^{R33Q} (20) and CASQ2^{DEL} (21), respectively, in permeabilized canine ventricular myocytes. Myocytes were infected with adenoviruses carrying the coding region of human CASQ2^{WT}, CASQ2^{R33Q} (20) or CASQ2^{DEL} proteins (21). Cells infected with a viral construct containing a short DNA segment served as controls for viral infection. As we reported previously (20, 21), ectopic expression of WT and R33Q mutant CASQ2 in myocytes resulted in an approximately 3-fold increase in total CASQ2 with no significant changes in native CASQ2 level. Additionally, expression of CASQ2^{DEL} caused no changes in the endogenous CASQ2 (Online Supplement, Fig 1). Permeabilized myocytes allow unrestricted access to the cytosolic compartments and have been used to study SR Ca release in different laboratories (6, 28). Saponin-permeabilized myocytes were kept in an internal solution containing 100 nM free [Ca] (0.05 mM EGTA). Under these conditions, myocytes generated periodic spontaneous discharges of [Ca]_{SR}, monitored at two optical channels as waves of cytosolic Ca elevations propagating across the myocytes and mirrored by reciprocal decreases in [Ca]_{SR}.

Ectopic expression of CASQ2^{WT} or either mutant CASQ2 protein resulted in profound changes in cytosolic and luminal Ca release signals compared to control (Fig. 1). The frequency of Ca waves was reduced and their cytosolic amplitude was increased in myocytes overexpressing CASQ2^{WT} as compared to control myocytes (Fig. 1; Fig 2A,B). At the same time, the baseline and maximum depletion (nadir) of [Ca]_{SR} at the peak of the waves in CASQ2^{WT} myocytes did not change although the rate of recovery of the [Ca]_{SR} was markedly slowed compared to control myocytes (Fig. 1; Fig. 2C,D,E). As we previously demonstrated (29), these effects of overexpressing WT CASQ2 are attributable to increased Ca buffering and increased amount of releasable Ca in the SR. Consistent with the arrhythmogenic nature of both CPVT mutations, the frequency of spontaneous waves was significantly higher in myocytes expressing either CASQ2^{R33Q} or CASQ2^{DEL} compared to control cells (Fig. 1; Fig. 2A). However, other characteristics of the waves were affected differently by the two CASQ2 variants, suggesting different underlying mechanisms. For example, the amplitude of cytosolic Ca waves was significantly reduced in CASQ2^{DEL} myocytes but increased in CASQ2^{R33Q} myocytes with respect to control (Fig. 1; Fig. 2B). Additionally, the recovery kinetics of [Ca]_{SR} were accelerated in CASQ2^{DEL}-expressing cells but were slowed in cells expressing CASQ2^{R33Q} or CASQ2^{WT} (Fig. 1; Fig. 2E). Furthermore, whereas CASQ2^{R33Q} caused a significant decrease in both baseline and nadir [Ca]_{SR}, CASQ2^{DEL} had no significant effect on these parameters of the [Ca]_{SR} signal (Fig. 1). Data on Fluo-5N fluorescence and estimated [Ca]_{SR} for the four experimental groups are summarized in Fig. 2C and D and Table 1. These disparate effects of the two CPVT mutants might be an indication that the mutations disrupt different aspects of CASQ2 function, specifically, its capacity to buffer SR Ca and to modulate RyR2 functional activity.

Local Ca release- and depletion signals.

To further investigate the effects of CASQ2 mutants on SR Ca handling we performed measurements of elemental Ca release events, or Ca sparks, along with the associated local [Ca] depletion signals in the SR (Fig. 3). These signals, also referred to as “blinks” (3), represent the decline in free [Ca] at individual jSR elements that are connected to the SR network through diffusion restricting pathways. Overexpression of CASQ^{WT} and CASQ^{R33Q} increased Ca spark amplitude, whereas expression of CASQ^{DEL} decreased Ca spark amplitude. The nadir of the local [Ca]_{SR} depletion signal in CASQ^{WT} or CASQ^{DEL}-expressing myocytes were similar to control (Fig. 3A,C,D; Table 2). At the same time, the rate of recovery of the local Ca depletion signals was slowed markedly by CASQ^{WT} and accelerated by CASQ^{DEL} (Fig. 3 A,B). In CASQ^{R33Q}-expressing cells the basal and nadir [Ca]_{SR} were lowered as compared to those in the other three groups (i.e. control, WT and DEL) (Fig. 3A,C,D; Table 2) and the rate of [Ca]_{SR} recovery was slowed similar to CASQ^{WT} overexpressing myocytes (Fig. 3A,B). These results are consistent with the effects of the CASQ2 variants upon SR Ca depletion signals during “global” Ca waves and present the first functional evidence that CASQ2 resides in jSR cisternae to facilitate and control Ca release from these sub-compartments. As in the case with the global Ca signals, the reduced Ca spark amplitude and accelerated local [Ca]_{SR} recovery in CASQ^{DEL} myocytes is indicative of reduced SR Ca buffering, whereas the reduced basal and nadir [Ca]_{SR} in CASQ^{R33Q} myocytes is consistent with altered RyR2 function. To further explore the effects of expressing the two CPVT mutants on SR Ca buffering, we examined the relationships between the cytosolic spark amplitude, which is a measure of Ca released, and the drop of [Ca]_{SR} for individual release events measured in myocytes from our four experimental groups. The resulting plot (Fig. 3E) reveals linear relationships with slopes roughly proportional to local SR Ca buffering. Both CASQ^{WT} and CASQ^{R33Q} increased buffering while CASQ^{DEL} decreased it. The finding that [Ca]_{SR} declined to the same lowest level suggests that Ca release terminates at a constant, threshold *free* luminal [Ca] despite profound differences in the amounts of releasable Ca and SR buffering strengths in the control, CASQ^{WT} and CASQ^{DEL} myocytes. Expression of CASQ^{R33Q} appears to reduce the threshold for Ca release termination by affecting RyR2 function. The mechanisms of alterations of SR Ca buffering and RyR2 function by CASQ^{DEL} and CASQ^{R33Q} were further pursued by studying the effects of these mutant proteins on CASQ2 polymerization and on interaction of CASQ2 with TRD.

Effects of expression of CPVT-associated CASQ2 mutants on CASQ2 polymerization.

It has been demonstrated by *in vitro* studies that the polymeric form of both skeletal and cardiac CASQ possesses higher Ca binding capacity than monomeric CASQ (15). To test the hypothesis that ectopic expression of CASQ^{DEL} reduced SR Ca binding capacity by impairing polymerization of CASQ2, we performed fluorescent label localization and FRET experiments using CASQ2 fusion constructs composed of either the WT or mutant forms of the protein conjugated with the fluorescent proteins CFP or YFP expressed in a heterologous system, 3T3 fibroblasts. These cells have no detectable levels of endogenous CASQ2 which would interfere with our FRET measurements by binding to the fusion constructs. We coexpressed WT CASQ2 conjugated with CFP (CASQ^{WT}-CFP) with the YFP-tagged CASQ2 variants CASQ^{WT}-YFP, CASQ^{DEL}-YFP or CASQ^{R33Q}-YFP. In the FRET experiments, CFP (illuminated at 458 nm) served as a donor and YFP served as acceptor and FRET efficiency was measured as a relative increase of CFP fluorescence at 475-500 nm after photobleaching YFP with unattenuated 515

nm laser. Representative images of 3T3 fibroblasts co-transfected with CASQ2^{WT}-CFP and CASQ2^{WT}-YFP, CASQ2^{DEL}-YFP or CASQ2^{R33Q}-YFP before and after acceptor photobleaching are shown in Fig. 4. Both CFP and YFP-tagged WT CASQ2 showed a characteristic distribution limited to well-defined puncta in the cells. Such punctate distribution of CASQ1 has been described previously and attributed to CASQ1 monomers aggregating into clusters of supramolecular complexes within the ER or SR in myotubes (14). Consistent with this view co-expressed CASQ2^{WT}-CFP and CASQ2^{WT}-YFP produced a highly efficient FRET manifest by increased brightness of CFP fluorescence following acceptor photodestruction.

CASQ2 polymerization is thought to be dependent on [Ca] such that polymerization is promoted at elevated [Ca] while monomers predominate at lower [Ca]. Therefore we investigated the effects of loading and depleting the ER Ca stores on both distribution of CASQ2 and FRET between CFP and YFP tagged CASQ2 monomers. As illustrated by Fig. 5A depletion of the ER stores by application of 1 μ M ionomycin in the presence of 5 mM EGTA resulted in a marked decrease in FRET efficiency. The Ca concentration dependence of FRET, obtained by using several different Ca concentrations in the incubation medium, was characterized by a sigmoidal function with EC₅₀ ~500 μ M and cooperativity of 1 (Fig. 5C). The Ca-dependence of FRET is in agreement with *in vitro* and *in situ* estimates of Ca binding to CASQ (10, 30) (EC₅₀~500 μ M).

It has been suggested that cyclical changes in CASQ2 polymerization may occur in cardiac myocytes on a beat to beat basis (15). We directly examined this possibility by assessing the rate of depolymerization of WT CASQ2 on lowering [Ca] using FRET measurements. Maximum FRET was obtained by exposing ionomycin-treated cells to 10 mM Ca; then Ca was removed (0 Ca) and FRET efficiency values determined at different time points (Fig 5D). As indexed by the time course of FRET decrease, CASQ2 depolymerization occurred with a time constant of ~18.1 min (Fig. 5D), which is too slow on the time scale of the cardiac cycle. Similar results were obtained when instead of using ionomycin, the ER stores of saponin-permeabilized cells were rapidly depleted by application of the IP₃ receptor agonist adenophostin (10 μ M) and the SERCA pump inhibitor thapsigargin (10 μ M) (not shown). Collectively, these results with expression of CASQ2^{WT} indicate that CASQ2 aggregates in cells and this process is Ca-dependent but apparently too slow to occur on the time scale of the cardiac cycle.

Cellular distribution and polymerization of CASQ2^{DEL} and CASQ2^{R33Q}.

The results obtained with coexpression of the CASQ2^{WT} and CASQ2^{DEL} constructs were markedly different from those obtained in cells expressing CASQ2^{WT} alone. Instead of the well-defined punctate labeling pattern observed in CASQ2^{WT}-expressing cells, cells coexpressing CASQ2^{WT} and CASQ2^{DEL} exhibited a much less defined and more diffuse labeling pattern (Fig. 4). A similar diffuse pattern was apparent for both CASQ2^{WT} and CASQ2^{DEL} (as revealed by CFP and YFP fluorescence) and has been described previously for CASQ1 mutants that lacked the ability to polymerize (14). Our results suggest that CASQ2^{DEL} is not only unable to self-polymerize but also acts in a dominant negative manner to disrupt the ability of CASQ2^{WT} to form multimolecular complexes. Consistent with these changes in fluorescence labeling, cells coexpressing CASQ2^{WT} and CASQ2^{DEL} did not exhibit a significant FRET signal irrespective of Ca presence. Moreover, adenovirus-mediated expression of CASQ2^{DEL} reduced energy transfer between CASQ2^{WT}-CFP and CASQ2^{WT}-YFP and altered the CASQ2^{WT} distribution pattern in fibroblasts (Fig. 4; Fig. 5B). The dispersive effect of the DEL mutant upon distribution of WT

CASQ2 was further confirmed in immunocytochemistry experiments with expression of untagged WT and DEL CASQ2 proteins (Online Supplement, Fig. 2).

In contrast to the effects of CASQ2^{DEL}, ectopic expression of CASQ2^{R33Q} exerted no discernible impact on CASQ2 distribution (Fig. 4). The ability to generate FRET and its Ca dependence was also generally preserved (Fig. 5A). In fact the Ca dependency of FRET between CASQ2^{WT} and CASQ2^{R33Q} exhibited a substantial leftward shift (EC_{50} 51 μ M, Fig. 5C). Taken together our results suggest that the reduced Ca buffering capacity of myocytes expressing CASQ2^{DEL} can be ascribed to disruption of CASQ2 polymerization required for high capacity Ca binding. These results also indicate that in contrast to CASQ2^{DEL}, ectopic expression of CASQ2^{R33Q} has minimal impact on CASQ2 polymerization, consistent with the view that this mutation affects SR Ca release by altering the activity of the RyR2 channel rather than by compromising CASQ2 Ca binding activity.

Interaction of CASQ2^{DEL} and CASQ2^{R33Q} with triadin.

It has been shown previously that CASQ2 modulates RyR2 function through interaction with TRD (17). To test the possibility that the CASQ2 mutations under study altered the ability of CASQ2 to interact with TRD, we carried out *in vitro* binding measurements using affinity chromatography (Fig 6). In agreement with previous reports (16), TRD interacted with WT CASQ2 in a Ca-dependent manner, i.e., the binding was stronger at 0 [Ca] (1 mM EGTA) than at 1 mM [Ca] (Fig. 6B,C). Although the mean values for CASQ2^{R33Q} binding to TRD showed a tendency to be lower as compared to those for CASQ2^{WT} in both the presence and absence of CaCl₂ these changes were not statistically significant (Fig. 6C). CASQ2^{DEL} exhibited no detectable binding to TRD in the presence (Fig. 6B) and absence of Ca (data not shown). Since this mutant lacks the entire C-terminal region, these results are consistent with the possibility that the TRD binding domain of CASQ2 resides in its C-terminal region as suggested for the skeletal isoform of the protein (31). These results also suggest that the effects of expression of CASQ2^{DEL} on myocyte Ca handling do not involve direct actions of the protein on the RyR2 channel complex. On the other hand, since the R33Q mutant is able to bind TRD, ectopic expression of this mutant may alter Ca handling by displacing endogenous CASQ2 from the RyR2 channel complex.

DISCUSSION.

In the present study, we compared the effects of expression of two recently identified CASQ2 variants DEL and R33Q associated with CPVT (20, 21), on local SR Ca signaling in cardiac myocytes. Ectopic expression of these CASQ2 variants altered myocyte Ca signaling through two different mechanisms: by disrupting CASQ2 polymerization required for high capacity Ca binding and by impairing the ability of CASQ2 to modulate RyR2 function. Our results demonstrated that CASQ2 polymerization is a critical factor in determining the buffering function of CASQ2 and provided new evidence for the role of luminal Ca and CASQ2 in termination of SR Ca release. These findings are summarized in Fig. 7.

CASQ2 as a local Ca buffer.

Classical EM studies demonstrated that skeletal and cardiac CASQ forms an electron-dense matrix in the lumen of the junctional SR, in the proximity of RyRs (12). However, the functional significance of this unique organization has not been clearly established. Our simultaneous

measurements of focal extra- and intra-SR Ca signals (i.e. Ca sparks and “blinks”) in myocytes expressing the WT and mutant CASQ2 have provided functional evidence for the ability of CASQ2 to buffer Ca locally, i.e. within individual junctional SR cisternae, confirming the idea that CASQ2 serves to concentrate Ca at the sites of SR Ca release to facilitate Ca signaling by RyR2s. In particular, our data showed that overexpression of WT CASQ2 increased both the amount of Ca released during a Ca spark and the time required for refilling of an individual jSR store following local Ca release indicative of enhanced Ca buffering within this structure (Fig. 3). At the same time, disrupting CASQ2 polymerization by expressing CASQ2^{DEL} resulted in reduced local Ca release and accelerated recovery of $[Ca]_{SR}$, consistent with reduced Ca buffering inside the jSR. Thus, polymerized CASQ2 within the jSR enables individual jSR cisternae to operate as functionally independent Ca storage- and release sites with their own reserve of releasable Ca. Since the amount of CASQ2 sequestered near the RyR2s is critical in determining the “quanta” of Ca released during elementary Ca release events, CASQ2 should be viewed as part of the Ca release unit along with the RyR2 clusters it is functionally and structurally associated with.

Cyclical changes in CASQ2 polymerization have been proposed to occur in cardiac myocytes and regulate the level of free intra-SR Ca on a beat-to-beat basis (15). This attractive hypothesis is based on *in vitro* effects of Ca as well as those of pH and potassium ions on CASQ2 structural transitions. However, our direct measurements of the time course of CASQ2 polymer disassembly using FRET indicated that this process is too slow (minutes rather than seconds) to occur on the time scale of the cardiac cycle (Fig. 5D).

Role of luminal Ca and CASQ2 in termination of local SR Ca release.

In addition to shedding new light on the role of CASQ2 as a local Ca buffer, our studies also yielded new evidence for the role of CASQ2 and luminal Ca in dynamic modulation of SR Ca release. We found that regardless of the amount of total Ca present in the SR, both global and local Ca release terminated always at a certain threshold free luminal $[Ca]$. For example, the local free $[Ca]_{SR}$ depletion signals during sparks fell to the same lowest value in myocytes expressing CASQ2^{WT} or CASQ2^{DEL} (Fig. 3). This occurred despite the fact that the amount of SR Ca buffering and total Ca released were increased by overexpression of CASQ2^{WT} but reduced by overexpression of CASQ2^{DEL}. Importantly, we were able to alter the $[Ca]_{SR}$ threshold for Ca release termination by disrupting interactions of CASQ2 with the RyR2 complex. This was achieved by expressing CASQ2^{R33Q} with a “gain in function” effects on Ca spark frequency (20), which not only reduced the basal $[Ca]_{SR}$ (due to increased SR Ca leak) but also lowered the nadir of Ca depletion signals during both global and local Ca release with respect to the other experimental groups (Fig 1; Fig. 2D; Fig. 3A,C,D; Table 1,2). These findings provide strong support for the hypothesis that changes in luminal Ca serve an important role in Ca release termination and that CASQ2 is involved in mediating the effects of luminal Ca on the RyR2 channel (17).

Modes of action of DEL and R33Q on SR Ca release.

In accord with our previous studies (21), ectopic expression of CASQ2^{DEL} in cardiac myocytes resulted in a marked decrease in the amplitude of spontaneous Ca transients and Ca sparks, thus revealing a pronounced dominant negative effect of the mutant upon the functional size of the Ca stores. In principle, such a dominant negative effect could be attributable to either impairment of

CASQ2 polymerization required for high capacity Ca binding and/or to disrupted interaction of CASQ2 with the RyR2 channel complex, leading to leaky RyR2s and depleted SR Ca stores. Based on several key pieces of experimental evidence we propose that CASQ2^{DEL} acted through the former rather than through the latter mechanism. Specifically, although expression of CASQ2^{DEL} reduced the intra-SR Ca buffering (as evidenced by accelerated recovery kinetics of $[Ca]_{SR}$ following SR Ca release) the steady-state free $[Ca]_{SR}$ was not altered (Fig. 1; Fig. 2C,E, Table 1). Since the steady-state $[Ca]_{SR}$ is determined by the balance between SR Ca uptake and leak the fact that this parameter was not affected in our experiments strongly suggests that CASQ2^{DEL} does not alter the functional activity of RyR2s. In accord with this conclusion, our *in vitro* binding experiments detected no physical interactions between CASQ2^{DEL} and TRD, the putative mediator of CASQ2's influence on the RyR2 channel (Fig. 6). At the same time, our fluorescent tag localization, immunocytochemistry and FRET experiments revealed that the mutant protein not only lacked the capacity of CASQ2 to self-polymerize but disrupted the ability of CASQ2^{WT} to form supramolecular complexes in a homologous expression system (Fig. 4; Fig 5A,B, Online Supplement Fig. 2). Since polymerized CASQ2 represents the high Ca binding capacity form of the protein (15) disruption of polymerization could account for the dominant negative effects of CASQ2^{DEL} on SR Ca storing capacity (Fig. 7, middle). Thus collectively, these findings suggest that expression of CASQ2^{DEL} alters myocytes Ca handling by disrupting CASQ2 polymerization.

In comparison, expression of CASQ2^{R33Q} increased the SR Ca leak and led to a reduction in *free* steady-state $[Ca]_{SR}$, without affecting SR Ca binding capacity, as evidenced by the lack of an effect upon recovery kinetics of $[Ca]_{SR}$ following SR Ca release (Fig. 1; Fig. 2C,E, Table 1) or intra-SR Ca buffering slope (Fig 3E). Additionally, based on the results of fluorescent labeled protein localization and FRET experiments, this mutant did not affect the ability of CASQ2 to polymerize (Fig. 4; Fig. 5A). CASQ2^{R33Q} also retained an ability to bind to TRD albeit less strongly than its WT counterpart (Fig. 6). Interestingly, despite its ability to physically associate with TRD, CASQ2^{R33Q} lacks the efficiency of CASQ2^{WT} to inhibit RyR2 function in lipid bilayers (20). Thus, the gain-of-function effects of this mutant on SR Ca release in CASQ2^{R33Q}-expressing myocytes could be ascribed to the mutant displacing endogenous CASQ2 with an inhibitory action from the RyR2 complex (Fig. 7, right).

Relevance to CPVT.

Based on our present as well as previous studies in myocytes we can distinguish two principal mechanisms as to how CASQ2 mutations lead to arrhythmogenic disturbances in Ca transients and electrical activity. Both mechanisms act by disrupting the normal control of RyR2s by luminal Ca and CASQ2 required for efficient turning off Ca release during the diastolic phase (Fig. 7, left). Shortened and reduced Ca signaling refractoriness results in spontaneous Ca release and arrhythmogenic DADs, as previously shown in myocytes expressing CPVT CASQ2 mutants, including R33Q and DEL (20, 21). In case of mutations that reduce CASQ2 abundance and/or Ca binding activity (DEL), shortened refractoriness is caused by premature recovery of $[Ca]_{SR}$ in the vicinity of RyR2s (Fig 7, middle). With mutations that disrupt CASQ2 interaction with RyR2 (via TRD, e.g. R33Q (20) and D307H (32)), the same effect is attributable to impaired ability of CASQ2 to act as a luminal Ca sensor i.e. inhibit RyR2 at low $[Ca]_{SR}$ (Fig. 7, right). SERCA activity is also an important factor in determining the rate of refilling of the SR

and hence the duration of luminal Ca dependent refractoriness (33), and stimulation of SERCA (via PLB) is likely to explain the dependence of arrhythmia on adrenergic stimulation.

In animal models of CPVT or clinical settings when only the mutant form of the protein is present (i.e. homozygous carriers), the two mechanisms affecting either the buffering or modulatory function of CASQ2 are likely to act in parallel to induce the CPVT phenotype. For example, a complete lack of CASQ2 would be expected to both alter intra-SR Ca buffering and directly affect RyR2 gating. Additionally, compensatory changes, including SR volume expansion (34) and upregulation of the SR Ca binding protein calreticulin (35) are also likely to influence manifestations of CPVT under chronic settings. Such compensatory changes along with differences in mutant protein expression levels (35) under conditions of chronic vs. acute settings are likely to account for the fact that CPVT is observed only in homozygous carriers despite the dominant negative effects of the mutants in our experiments. Finally, it is to be noted that although our results provide insights into molecular and subcellular basis of CPVT, it remains to be defined how abnormalities in Ca homeostasis and DADs in a single myocardial cell cause an arrhythmia in the whole heart. Recently, evidence for an important role of myocardial conduction system, namely Purkinje cells, in arrhythmogenesis in CPVT has been presented (36).

SOURCES OF FUNDING.

This work was supported by the American Heart Association (D.T., S. V-K.), VEGA 2/0102/08 (ZK), Telethon grant No. GGP04066 (PV), and National Institutes of Health Grants HL074045 and HL063043 (S.G.).

DISCLOSURES.

None.

REFERENCES.

- [1] Bers, D.M. 2001. Excitation-Contraction Coupling and Cardiac Contractile Force. Dordrecht, The Netherlands: Kluwer Academic Publishers.
- [2] Shannon, T.R., T. Guo, and D.M. Bers. 2003. Ca²⁺ scraps: local depletions of free [Ca²⁺] in cardiac sarcoplasmic reticulum during contractions leave substantial Ca²⁺ reserve. *Circ. Res.* 93:40-45.
- [3] Brochet, D.X., D. Yang, A. Di Maio, W.J. Lederer, C. Franzini-Armstrong, and H. Cheng. 2005. Ca²⁺ blinks: rapid nanoscopic store calcium signaling. *Proc. Natl. Acad. Sci. USA.* 102:3099-3104.
- [4] Lukyanenko, V., T.F. Wiesner, and S. Gyorke. 1998. Termination of Ca²⁺ release during Ca²⁺ sparks in rat ventricular myocytes. *J. Physiol.* 507:667-677.
- [5] Sham, J.S., L.S. Song, Y. Chen, L.H. Deng, M.D. Stern, E.G. Lakatta, and H. Cheng. 1998. Termination of Ca²⁺ release by a local inactivation of ryanodine receptors in cardiac myocytes. *Proc. Natl. Acad. Sci. USA.* 95:15096–15101.
- [6] Terentyev, D., S. Viatchenko-Karpinski, H.H. Valdivia, A.L. Escobar, and S. Gyorke. 2002. Luminal Ca²⁺ controls termination and refractory behavior of Ca²⁺-induced Ca²⁺ release in cardiac myocytes. *Circ. Res.* 91:414-420.
- [7] Sobie, E.A., K.W. Dilly, J. dos Santos Cruz, W.J. Lederer, and M.S. Jafri. 2002. Termination of cardiac Ca(2+) sparks: an investigative mathematical model of calcium-induced calcium release. *Biophys. J.* 83:59-78.
- [8] Szentesi, P., C. Pignier, M. Egger, E.G. Kranias, and E. Niggli. 2004. Sarcoplasmic reticulum Ca²⁺ refilling controls recovery from Ca²⁺-induced Ca²⁺ release refractoriness in heart muscle. *Circ. Res.* 95:807-813.
- [9] Zima, A.V., E. Picht, D.M. Bers, and L.A. Blatter. 2008. Partial inhibition of sarcoplasmic reticulum Ca release evokes long-lasting Ca release events in ventricular myocytes: role of luminal Ca in termination of Ca release. *Biophys. J.* 94:1867-1879.
- [10] Mitchell, R.D., H.K. Simmerman, and L.R. Jones. 1988. Ca²⁺ binding effects on protein conformation and protein interactions of canine cardiac calsequestrin. *J. Biol. Chem.* 263:1376-1381.
- [11] Beard, N.A., D.R. Laver, and A.F. Dulhunty. 2004. Calsequestrin and the calcium release channel of skeletal and cardiac muscle. *Prog. Biophys. Mol. Biol.* 85:33-69.
- [12] Franzini-Armstrong, C., L. Kenney, and E. Varriano-Marston. 1987. The structure of calsequestrin in triads of vertebrate skeletal muscle: a deep-etch study. *J. Cell. Biol.* 105:45-56.
- [13] Wang, S., W.R. Trumble, H. Liao, C.R. Wesson, A.K. Dunker, and C.H. Kang. 1998. Crystal structure of calsequestrin from rabbit skeletal muscle sarcoplasmic reticulum. *Nat. Struct. Biol.* 5:476-483.
- [14] Gatti, G., S. Trifari, N. Mesaali, J.M. Parker, M. Michalak, and J. Meldolesi. 2001. Head-to-tail oligomerization of calsequestrin: a novel mechanism for heterogeneous distribution of endoplasmic reticulum luminal proteins. *J. Cell. Biol.* 154:525-534.

- [15] Park, H., I.Y. Park, E. Kim, B. Youn, K. Fields, A.K. Dunker, and C. Kang. 2004. Comparing skeletal and cardiac calsequestrin structures and their calcium binding: a proposed mechanism for coupled calcium binding and protein polymerization. *J. Biol. Chem.* 279:18026-18033.
- [16] Zhang, L., J. Kelley, G. Schmeisser, Y.M. Kobayashi, and L.R. Jones. 1997. Complex formation between junctin, triadin, calsequestrin, and the ryanodine receptor. Proteins of the cardiac junctional sarcoplasmic reticulum membrane. *J. Biol. Chem.* 272:23389-23397.
- [17] Gyorke, I., N. Hester, L.R. Jones, and S. Gyorke. 2004. The role of calsequestrin, triadin, and junctin in conferring cardiac ryanodine receptor responsiveness to luminal calcium. *Biophys. J.* 86:2121-2128.
- [18] Lahat, H., E. Pras, T. Olender, N. Avidan, E. Ben-Asher, O. Man, E. Levy-Nissenbaum, A. Khoury, A. Lorber, B. Goldman, D. Lancet, and M. Eldar. 2001. A missense mutation in a highly conserved region of CASQ2 is associated with autosomal recessive catecholamine-induced polymorphic ventricular tachycardia in Bedouin families from Israel. *Am. J. Hum. Genet.* 69:1378–1384.
- [19] Postma, A.V., I. Denjoy, T.M. Hoorntje, J.M. Lupoglazoff, A. Da Costa., P. Sebillon, M.M. Mannens, A.A. Wilde, and P. Guicheney. 2002. Absence of calsequestrin 2 causes severe forms of catecholaminergic polymorphic ventricular tachycardia. *Circ. Res.* 91:e21–e26.
- [20] Terentyev, D., A. Nori, M. Santoro, S. Viatchenko-Karpinski, Z. Kubalova, I. Gyorke, R. Terentyeva, S. Vedamoorthyrao, N.A. Blom, G. Valle, C. Napolitano, S.C. Williams, P. Volpe, S.G. Priori, and S. Gyorke. 2006. Abnormal interactions of calsequestrin with the ryanodine receptor calcium release channel complex linked to exercise-induced sudden cardiac death. *Circ. Res.* 98:1151-1158.
- [21] di Barletta, M.R., S. Viatchenko-Karpinski, A. Nori, M. Memmi, D. Terentyev, F. Turcato, G. Valle, N. Rizzi, C. Napolitano, S. Gyorke, P. Volpe, and S.G. Priori. 2006. Clinical phenotype and functional characterization of CASQ2 mutations associated with catecholaminergic polymorphic ventricular tachycardia. *Circulation.* 114:1012-1019.
- [22] Terentyev, D., S. Viatchenko-Karpinski, I. Gyorke, P. Volpe, S.C. Williams, and S. Gyorke. 2003. Calsequestrin determines the functional size and stability of cardiac intracellular calcium stores: Mechanism for hereditary arrhythmia. *Proc. Natl. Acad. Sci. USA.* 100:11759-11764.
- [23] Viatchenko-Karpinski, S., D. Terentyev, I. Gyorke, R. Terentyeva, P. Volpe, S.G. Priori, C. Napolitano, A. Nori, S.C. Williams, and S. Györke. 2004. Abnormal calcium signaling and sudden cardiac death associated with mutation of calsequestrin. *Circ. Res.* 94:471-477.
- [24] Kubalova, Z., D. Terentyev, S. Viatchenko-Karpinski, Y. Nishijima, I. Gyorke, R. Terentyeva, D.N. da Cunha, A. Sridhar, D.S. Feldman, R.L. Hamlin, C.A. Carnes, and S. Györke. 2005. Abnormal intrastore calcium signaling in chronic heart failure. *Proc. Natl. Acad. Sci. USA.* 102:14104-14109.
- [25] Saito, A., S. Seiler, A. Chu, and S. Fleischer. 1984. Preparation and morphology of sarcoplasmic reticulum terminal cisternae from rabbit skeletal muscle. *J. Cell. Biol.* 99:875-885.

- [26] Lowry, O.H., N.J. Roawbrough, A.L. Farr, and R.J. Randall. 1951. Protein measurement with the Folin phenol reagent. *J. Biol. Chem.* 193: 265–275.
- [27] Guo, W., A.O. Jorgensen, L.R. Jones, and K.P. Campbell. 1996. Biochemical characterization and molecular cloning of cardiac triadin. *J. Biol. Chem.* 271:458-465.
- [28] Zima, A.V., J.A. Copello, and L.A. Blatter. 2004. Effects of cytosolic NADH/NAD(+) levels on sarcoplasmic reticulum Ca(2+) release in permeabilized rat ventricular myocytes. *J Physiol.* 555:727-741.
- [29] Kubalova, Z., I. Gyorke, R. Terentyeva, S. Viatchenko-Karpinski, D. Terentyev, S.C. Williams, and S. Gyorke. 2004. Modulation of cytosolic and intra-sarcoplasmic reticulum calcium waves by calsequestrin in rat cardiac myocytes. *J. Physiol.* 561:515-524.
- [30] Guo, T., X. Ai, T.R. Shannon, S.M. Pogwizd, and D.M. Bers. 2007. Intra-sarcoplasmic reticulum free [Ca²⁺] and buffering in arrhythmogenic failing rabbit heart. *Circ. Res.* 101:802-810.
- [31] Shin, D.W., J. Ma, and D.H. Kim. 2000. The asp-rich region at the carboxyl-terminus of calsequestrin binds to Ca(2+) and interacts with triadin. *FEBS. Lett.* 486:178-182.
- [32] Houle, T.D., M.L. Ram, and S.E. Cala. 2004. Calsequestrin mutant D307H exhibits depressed binding to its protein targets and a depressed response to calcium. *Cardiovasc. Res.* 64:227-233.
- [33] Szentesi, P., C. Pignier, M. Egger, E.G. Kranias, and E. Niggli. 2004. Sarcoplasmic reticulum Ca²⁺ refilling controls recovery from Ca²⁺-induced Ca²⁺ release refractoriness in heart muscle. *Circ Res.* 95:807-813.
- [34] Knollmann, B.C., N. Chopra, T. Hlaing, B. Akin, T. Yang, K. Etensohn, B.E. Knollmann, K.D. Horton, N.J. Weissman, I. Holinstat, W. Zhang, D.M. Roden, L.R. Jones, C. Franzini-Armstrong, and K. Pfeifer. 2006. Casq2 deletion causes sarcoplasmic reticulum volume increase, premature Ca²⁺ release, and catecholaminergic polymorphic ventricular tachycardia. *J. Clin. Invest.* 116:2510-2520.
- [35] Song, L., R. Alcalai, M. Arad, C.M. Wolf, O. Toka, D.A. Conner, C.I. Berul, M. Eldar, C.E. Seidman, and J.G. Seidman. 2007. Calsequestrin 2 (CASQ2) mutations increase expression of calreticulin and ryanodine receptors, causing catecholaminergic polymorphic ventricular tachycardia. *J. Clin. Invest.* 117:1814-1823.
- [36] Cerrone, M., S.F. Noujaim, E.G. Tolkacheva, A. Talkachou, R. O'Connell, O. Berenfeld, J. Anumonwo, S.V. Pandit, K. Vikstrom, C. Napolitano, S.G. Priori, and J. Jalife. 2007. Arrhythmogenic mechanisms in a mouse model of catecholaminergic polymorphic ventricular tachycardia. *Circ Res.* 101:1039-1048.

Table 1.

	F _{SR}		F _{SR} /F _{SRmax}		[Ca] _{SR} (mM)	
	Baseline	Nadir	Baseline	Nadir	Baseline	Nadir
Control	440±42	171±28	0.72±0.07	0.28±0.02	1.04±0.11	0.16±0.02
WT	364±54	138±16	0.66±0.09	0.25±0.01	0.78±0.15	0.13±0.01
DEL	416±20	162±12	0.69±0.03	0.27±0.01	0.88±0.07	0.15±0.01
R33Q	224 ±28* [†]	104±16* [†]	0.43±0.05* [†]	0.19±0.02* [†]	0.30±0.08* [†]	0.09±0.01* [†]

Parameters of Global intra-SR Ca Depletion Signals.

Global intra-SR Fluo-5N signals and estimated [Ca]_{SR} in permeabilized myocytes infected with control adenovirus and adenoviral constructs encoding WT CASQ2 and DEL and R33Q CASQ2 mutants. $F_{SR} = F - F_{CAFF}$; $F_{SRmax} = F_{max} - F_{CAFF}$; $[Ca]_{SR} = K_d(F_{SR}) / (F_{SRmax} - F_{SR})$; where K_d was 400 μ M (2). * Significantly different if compared with control or [†] if compared with WT, $P < 0.05$, one way ANOVA, n of waves from 14 to 18, n of cells from 6 to 10.

Table 2.**Parameters of Local intra-SR Ca Depletion Signals.**

	F_{SR}		F_{SR}/F_{SRmax}		$[Ca]_{SR}(mM)$	
	Baseline	Nadir	Baseline	Nadir	Baseline	Nadir
Control	370±15	256±8	0.74±0.03	0.51±0.01	1.12±0.13	0.42±0.01
WT	376±47	270±38	0.75±0.09	0.54±0.08	1.22±0.25	0.48±0.09
DEL	401±19	287±14	0.73±0.03	0.52±0.03	1.08±0.16	0.45±0.05
R33Q	202±20* [†]	128±12* [†]	0.47±0.05* [†]	0.31±0.03* [†]	0.37±0.12* [†]	0.18±0.03* [†]

Local intra-SR Fluo-5N signals and estimated $[Ca]_{SR}$ in permeabilized myocytes infected with control adenovirus and adenoviral constructs encoding WT CASQ2 and DEL and R33Q CASQ2 mutants. $F_{SR}=F-F_{CAFF}$; $F_{SRmax}=F_{max}-F_{CAFF}$; $[Ca]_{SR} = K_d(F_{SR})/(F_{SRmax}-F_{SR})$; where K_d was 400 μM (2). * Significantly different if compared with control or [†] if compared with WT, $P<0.05$, one way ANOVA, n of blinks from 13 to 16, number of cells from 8 to 13.

FIGURE LEGENDS.**Figure 1.****Simultaneous measurement of [Ca] changes during spontaneous Ca waves in the cytosolic and SR luminal compartments, using the Ca indicators Rhod-2 and Fluo-5N.**

Representative images of Ca waves and intra-SR [Ca] recorded in permeabilized dog ventricular myocytes overexpressing WT or mutant forms of CASQ2 (48 hours after adenoviral infection). Traces represent time-dependent profiles of cytosolic Rhod-2 and luminal Fluo-5N signals. Spontaneous Ca waves were induced by lowering [EGTA] from 200 μ M to 50 μ M (PCa7) in the internal solution.

Figure 2.**Characteristics of spontaneous cytosolic and intra-SR Ca waves.**

A,B,C,D,E, Pooled data in control myocytes and in myocytes overexpressing WT or mutant forms of CASQ2; Values of spontaneous Ca wave frequency (A); Cytosolic Ca wave amplitude (B); baseline Fluo-5N fluorescence (C); nadir Fluo-5N fluorescence during intra-SR Ca waves (D); time constant of Fluo-5N fluorescence recovery of after SR Ca waves. *Significantly different when compared with control or † when compared to cells overexpressing CASQ^{WT} at P<0.05, one way ANOVA, n of waves from 8 to 14, n of cells from 6 to 10.

Figure 3.**Simultaneous measurement of [Ca] changes during spontaneous Ca sparks in the cytosolic and SR luminal compartments with the Ca indicators Rhod-2 and Fluo-5N.**

A, Representative images of Ca sparks (upper panel) and local intra-SR [Ca] depletion signals (“blinks”) recorded simultaneously with Rhod-2 and Fluo-5N, respectively, in permeabilized canine ventricular myocytes overexpressing WT or mutant forms of CASQ2 (48 hours after adenoviral infection). Traces at the bottom represent time-dependent profiles of Rhod-2 and Fluo-5N signals; B, Pooled data for the time constant of recovery of intra-SR Ca depletion signals in control myocytes and in myocytes expressing WT or mutant forms of CASQ2; C, Pooled data for the nadir of intra SR local [Ca] depletion signals in the same groups of cells as in B. * Significantly different when compared with myocytes infected with control virus or † when compared with myocytes overexpressing CASQ^{WT} at P<0.05, one way ANOVA, n of blinks from 13 to 16, n of cells from 8 to 13. D, Histogram presentation of the data for the nadir of intra SR [Ca] depletion signals. E, relationships between cytosolic Ca spark amplitude and the amplitude of the corresponding [Ca]_{SR} depletion signal ($F_{\text{Basal}}-F_{\text{Nadir}}$) for individual pairs of events measured in control cells and in cells expressing the DEL, WT and R33Q CASQ2 variants, respectively. The data are fit by a linear regression (solid lines) with slopes of 6.8, 2.6, 12.1 and 13.4 for Control and the DEL, WT and R33Q CASQ2 variants, respectively.

Figure 4.**Acceptor photobleaching experiments in fibroblasts coexpressing CASQ2 WT-CFP fusion protein with WT or mutant forms of CASQ2 fused with YFP.**

Representative confocal images of CFP and YFP fluorescence acquired from fibroblasts co-transfected with CASQ2^{WT}-CFP and CASQ2^{WT}-YFP (A), CASQ^{R33Q}-YFP (B) or CASQ2^{DEL}-YFP (C) fusion constructs before and after photodestruction of YFP. Panel D shows cells expressing the CASQ2^{WT}-CFP/CASQ2^{WT}-YFP FRET pair together with the adenovirally

delivered CASQ2^{DEL} mutant. All measurements were performed 36-48 hrs after transfection of cells with fusion constructs and infection with the adenoviral constructs.

Figure 5.

Polymerization of WT and mutant CASQ2s in living cells.

A, Pooled data for FRET efficiency in 3T3 fibroblasts coexpressing WT and mutant CASQ2 at 0 [Ca] (5 mM EGTA in the solution), or in the presence of 10 mM [Ca] (n from 18 to 28). Cells were exposed to 1 μ M of ionomycin. B, Pooled data for FRET efficiency in cells expressing WT CASQ2 CFP/YFP infected with adenoviral Ad-CASQ2^{WT} or Ad-CASQ2^{DEL} constructs at 10 mM [Ca] (n=14 and 15 respectively). C, Pooled data for efficiency of FRET between CASQ2^{WT}-CFP and CASQ2^{WT}-YFP or CASQ2^{R33Q}-YFP at different Ca concentrations. Data points (n from 18 to 24) were fitted using logistic functions with EC₅₀ values 509 and 51 μ mol/L for FRET to CASQ2^{WT} and CASQ2^{R33Q}, respectively. D, Time-dependent changes in FRET efficiency following application of 10 mM [Ca] (black triangles) or 0 [Ca] (5 mM EGTA, white circles) to fibroblasts in the presence of 1 μ M ionomycin. Data presented as mean \pm s.e.; n from 14 to 23. Data for 0 [Ca] were fitted with a single exponential function with time constant of 18.1 min.

Figure 6.

In vitro binding of TRD with either WT or mutant forms of T7-tagged CASQ2.

Purified CASQ2 affinity beads were incubated with CHAPS-solubilised cardiac heavy SR vesicles (100 μ g) in the presence of 1 mM CaCl₂ (panels A and B). After washing several times, bound proteins were eluted by SDS-sample buffer, subjected to SDS-PAGE and partly stained with Coomassie blue (Panel A, where grey arrowheads point to CASQ2) and partly transferred to a nitrocellulose sheet and immunostained with anti-TRD antibodies (Panel B, where TRD ψ and TRD δ indicate glycosylated and unglycosylated forms of TRD, respectively). Key to lanes: 1, CASQ2^{WT} affinity beads; 2, CASQ2^{R33Q} affinity beads; 3, CASQ2^{DEL} affinity beads; 4, Blank, affinity beads without any sample. Molecular mass standards are indicated by arrowheads on the right-hand side. Panel C summarizes densitometric data obtained for CASQ2^{WT} and CASQ2^{R33Q} in the presence of either 1 mM CaCl₂ (n=5) or 1 mM EGTA (n=4).

Figure 7.

Disruption of Ca storing and regulatory functions of CASQ2 by the CPVT CASQ2 mutants DEL and R33Q.

CASQ2 is present in the junctional SR in two forms (left-hand scheme): polymeric CASQ2 with high Ca binding capacity serves as a Ca storage site and controls [Ca]_{SR} in the vicinity of RyR2; monomeric CASQ2 regulates RyR2 activity in a [Ca]_{SR}-dependent manner (through binding to TRD). Ca release by RyR2s results in partial depletion of [Ca]_{SR} and the release is terminated at a certain threshold [Ca]_{SR} ([Ca]_{SRT}); Following their deactivation, RyR2s stay refractory until the jSR is refilled with Ca, a process that is influenced by CASQ2 Ca buffering capacity. Expression of CASQ2^{DEL} disrupts CASQ2 polymerization and reduces SR Ca buffering without altering interactions of WT CASQ2 with the RyR2 complex (middle). This results in accelerated recovery of [Ca]_{SR} and hence shortened restitution from luminal-Ca dependent deactivation that follows SR Ca release. Expression of CASQ2^{R33Q} displaces WT CASQ2 from the RyR2 complex without interfering with polymerization and Ca buffering (right). This impairs the ability of

CASQ2 to act as a luminal Ca sensor, i.e. inhibit RyR2 activity at low luminal Ca, resulting in lowered $[Ca]_{SRT}$ and shortened Ca signaling refractoriness. Thus, both CPVT mutant proteins act by disrupting normal control of RyR2 by CASQ2 and luminal Ca required for efficient turning of Ca release during the diastolic phase.

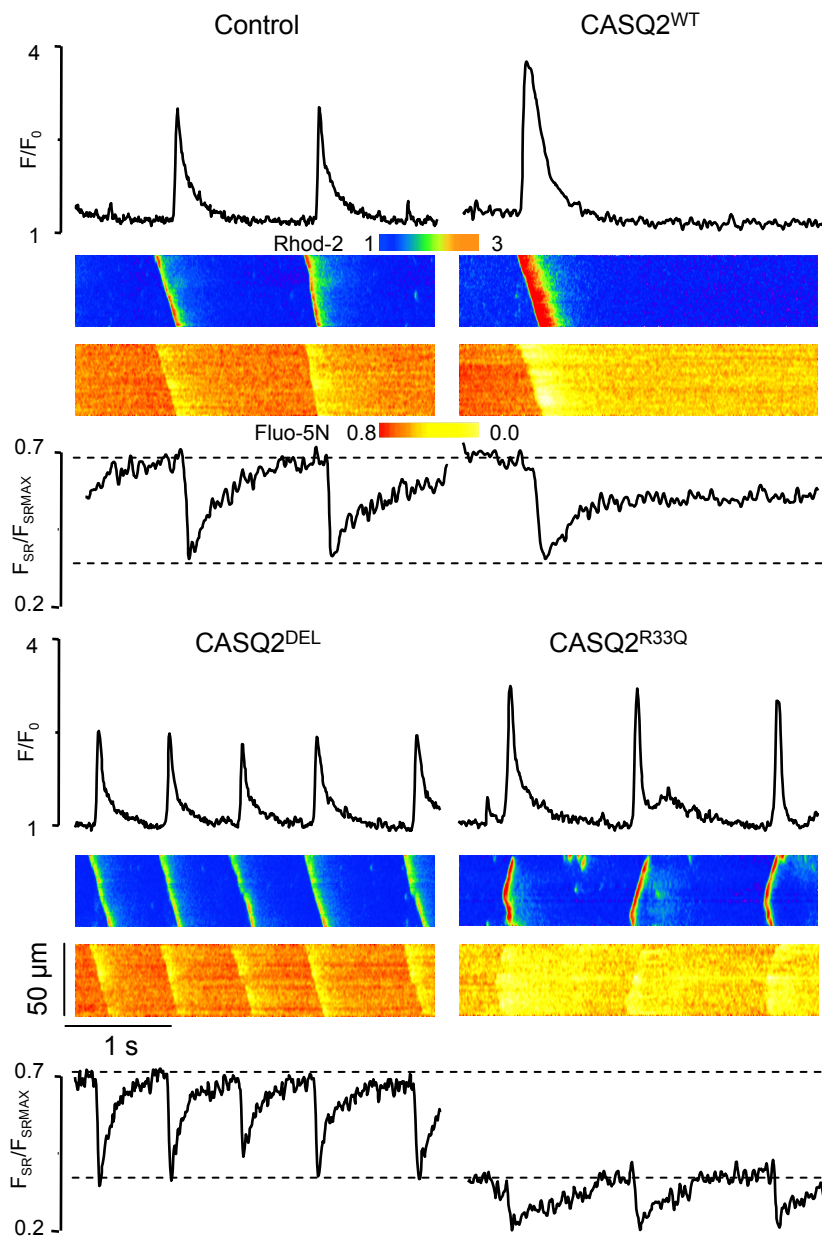


Figure 1

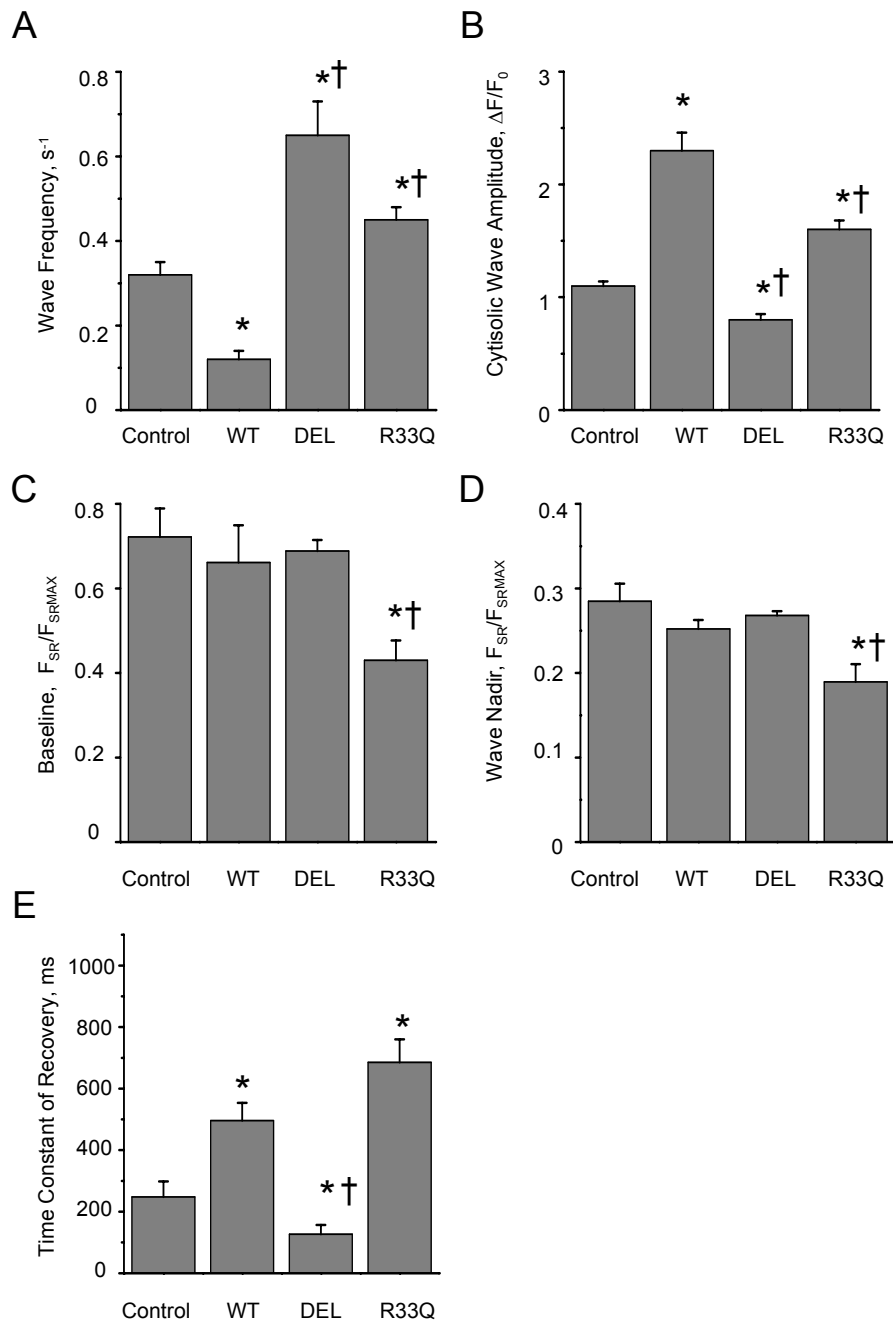


Figure 2

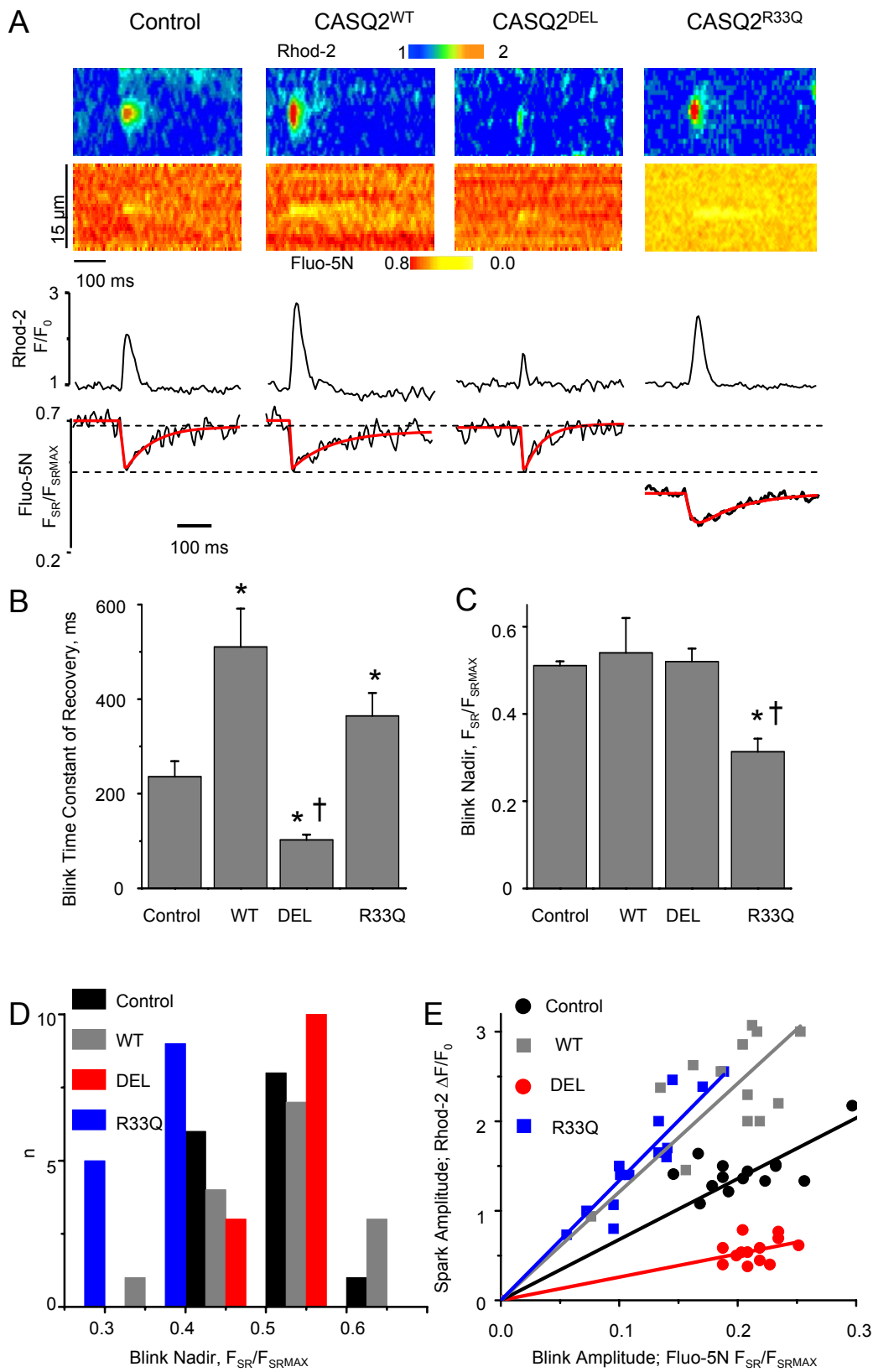


Figure 3

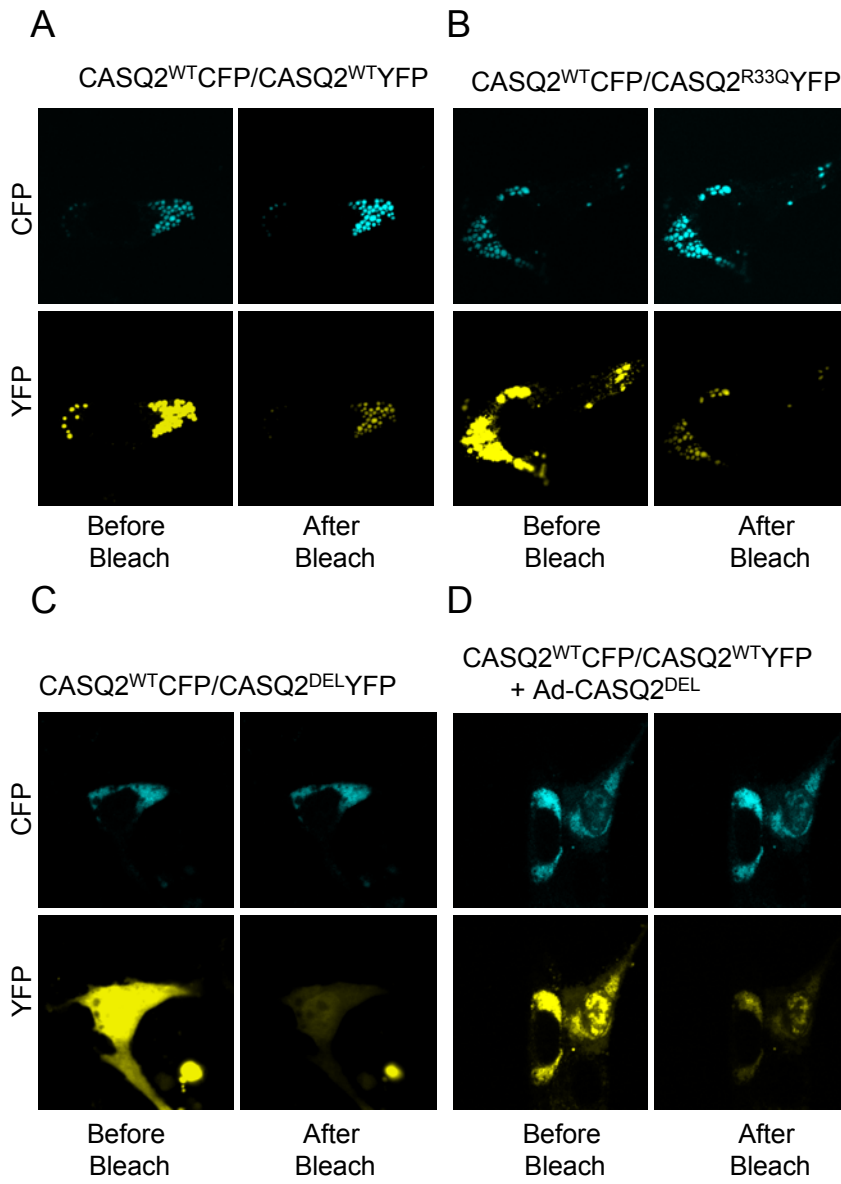


Figure 4

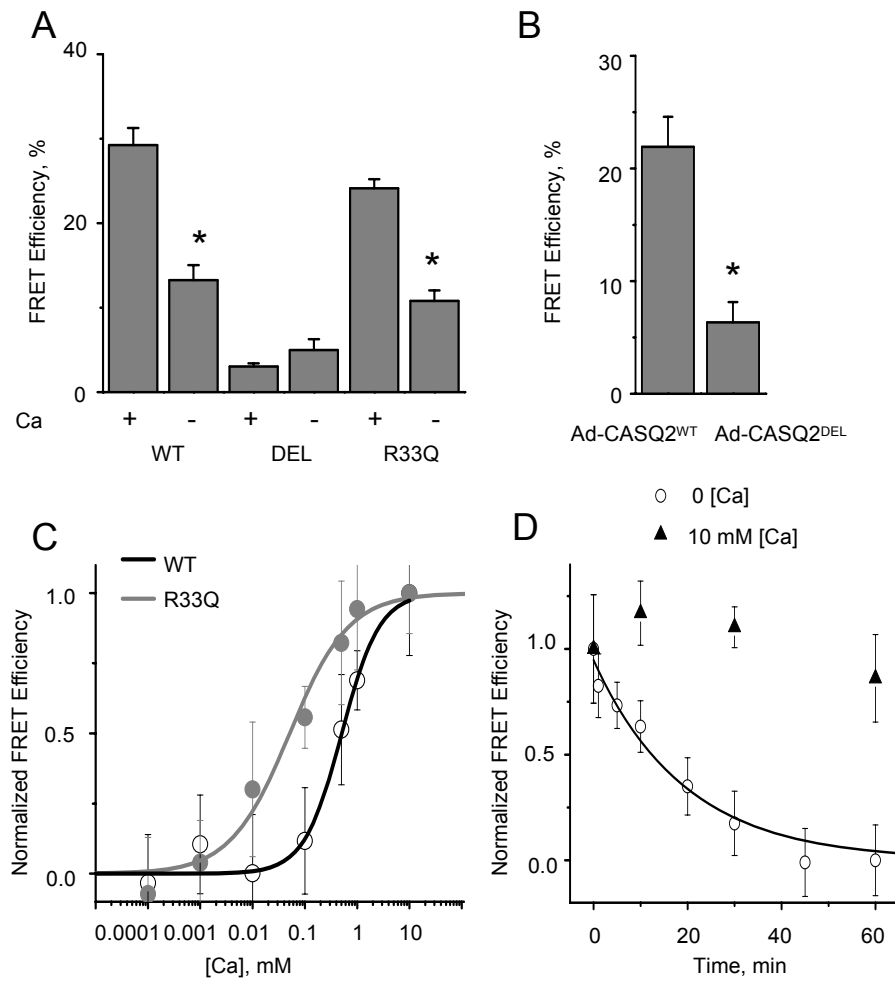


Figure 5

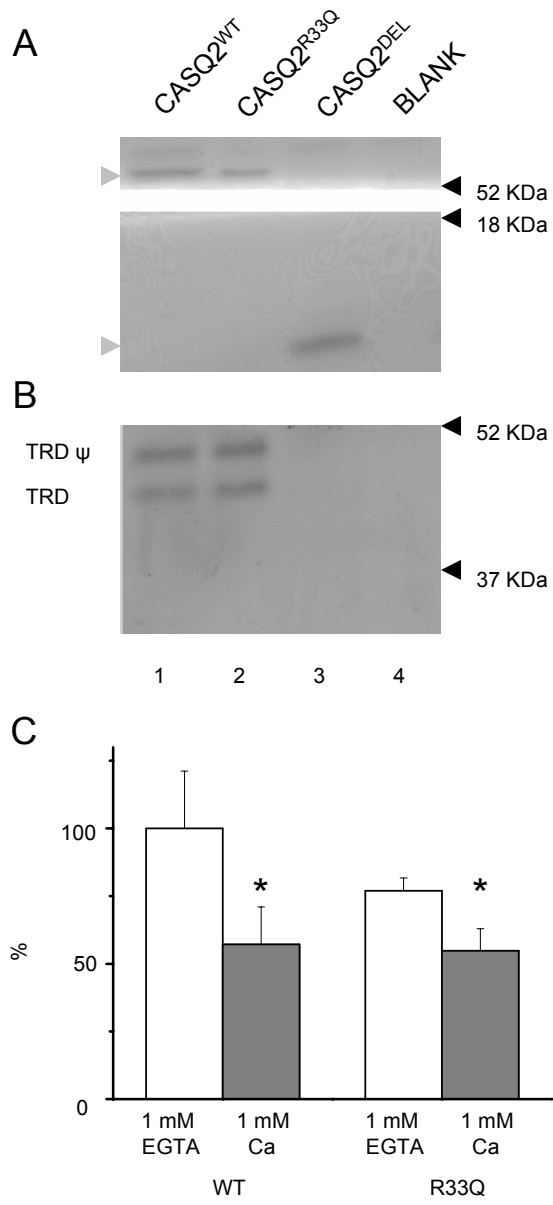


Figure 6

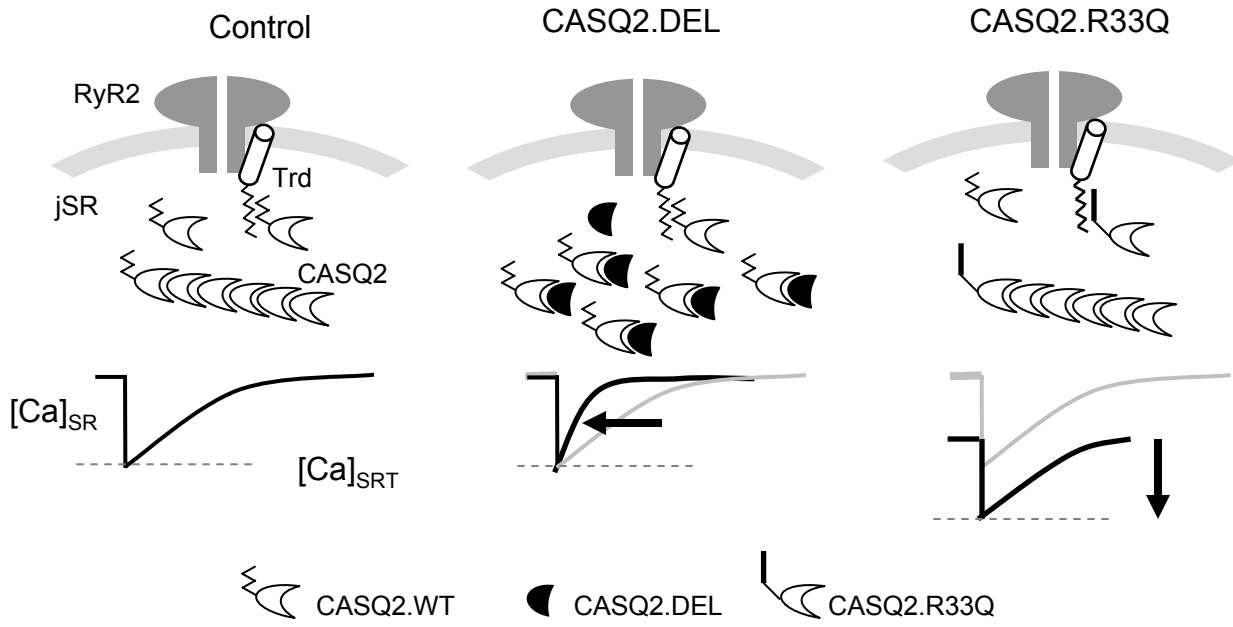


Figure 7